Journal of Kerman University of Medical Sciences

JKMU

Journal of Kerman University of Medical Sciences, 2018; 25 (3): 243-254

Destruction of Recombinant Tissue Plasminogen Activator (rtPA) -Loaded Echogenic Liposomes under Dual Frequency Sonication

Mosayyeb Mobasheri, M.Sc. [1], Manijhe Mokhtari-Dizaji, Ph.D. [2], Tayebeh Toliyat, Ph.D. [3], Masoud Mehrpour, MD [4]

1- Department of Medical Physics, Faculty of Medical Sciences, Tarbiat Modares University, Tehran, Iran

2- Professor, Department of Medical Physics, Faculty of Medical Sciences, Tarbiat Modares University, Tehran, Iran (Corresponding author; mokhtarm@modares.ac.ir)

3- Associate Professor, Department of Pharmaceutics, Faculty of Pharmacy, Tehran University of Medical Sciences, Tehran, Iran

4- Associate Professor, Department of Neurology, Firoozgar Hospital, Firoozgar Clinical Research Development Center (FCRDC), Iran University of Medical Sciences (IUMS), Tehran, Iran

Received: 4 April, 2018 Accepted: 26 June, 2018

ARTICLE INFO

Article type:
Original Article

Keywords:
Echogenic liposomes
Destruction
Fragmentation
Acoustically driven diffusion

Abstract

Background: Echogenic liposomes (ELIPs) encapsulate drugs and gas bubbles within lipid vesicles. The destruction of ELIPs in response to MHz and kHz ultrasound waves has been studied previously. Applying ultrasound above a certain threshold causes encapsulated gas bubbles destruct rapidly by fragmentation or more slowly by acoustically driven diffusion. This study compares the destruction of recombinant tissue plasminogen activator (rtPA) -loaded echogenic liposomes using three frequency protocols: 130 kHz, 1 MHz and dual (130 kHz + 1 MHz).

Method: In gel phantom, ELIPs were imaged by diagnostic ultrasound system and simultaneously destructive ultrasonic fields were applied at different intensities in each protocol. Images were analyzed.

Results: According to the results, 80% decline in MGV (mean of gray value) relative to initial MGV was associated with ELIPs fragmentation. At 130 kHz, results showed an 80% decline in MGV and fragmentation happened at all applied ultrasound intensities (0.01 W/cm^2 as fragmentation threshold). In MHz and dual protocols, on average, less than 50% decline in MGV was observed which indicated an acoustically driven diffusion.

Conclusion: Our study shows that kHz protocol fragments ELIPs more effectively than other two protocols. For better results, dual frequency protocols need optimized combination of frequencies and phases.

Citation: Mobasheri M, Mokhtari-Dizaji M, Toliyat T, Mehrpour M. Destruction of Recombinant Tissue Plasminogen Activator (rtPA) -Loaded Echogenic Liposomes under Dual Frequency Sonication. Journal of Kerman University of Medical Sciences, 2018; 25 (3): 243-254.

Introduction

Destruction of encapsulated bubbles by ultrasound energy is of interest in both diagnostic and therapeutic applications including flash echo, destruction/reperfusion imaging (1, 2) and drug delivery (3). Three mechanisms have been associated with ultrasound-induced bubble destruction (4): diffusion, acoustically driven diffusion and fragmentation. In diffusion, concentration gradient of gas causes mass transfer to surrounding medium. Interaction of bubble and acoustic wave changes bubble volume and concomitant changes in the

concentration gradient results in acoustically driven diffusion. In fragmentation, the bubble oscillations become unstable and some fragments separate from it within microseconds. Fragmentation is probably due to surface instabilities generated during the collapse of bubble (5).

Different methods have been used in order to investigate bubble destruction: signal processing methods based on detecting the acoustic emissions from bubbles (4, 6), observing bubbles using optical microscope (4,7,8) and loss of echogenity on B-mode images (9, 10, 11). In acoustical studies, pressure waves emitting from destructing bubbles were studied. In optical studies, shape variations of one bubble were observed and bubble was divided into some fragments. In B-mode images, due to mismatch of the acoustic impedance of gas and surrounding liquids, bubbles are echogenic. Bubble destruction causes the release of gas to surrounding medium and loss of echogenity (10). In fragmentation, loss of echogenity is fast (microsecond) and in acoustically driven diffusion it is slower (9, 10).

Interaction of a bubble and acoustic wave mainly depends on pressure amplitude, frequency of wave and also on the radius of bubble (its natural frequency) (12). Best yield (large bubble radius oscillations) happens when the radiation frequency matches the natural frequency of bubble. Low-frequency (kHz) radiation induces cavitation at low pressure amplitudes and for wide distribution of bubble natural frequencies (13). For equally sized and shaped transducers, relative to MHz waves, kHz waves have larger spatial pulse length and lower attenuation. Thus, low frequency waves (kHz) sonicate large volumes of tissues. For more control over sonication volume, some studies have used multi frequency waves (MHz- kHz or two neighboring kHz frequencies) and they showed an increased cavitation activity and bubble destruction (14). Sokka et al. (15) studied the effect of dual frequency radiation on microbubbles and the results showed that dual-frequency methods decrease the cavitation threshold. Hasanzadeh et al. (16) showed that dual frequency radiations enhance subharmonic amplitude of signal (acoustic characteristics of stable cavitation). Using terephthalic acid dosimetry (characteristics of inertial cavitation), Barati et al. (17) showed synergetic enhancement of inertial cavitation activity by using dual frequency exposures (150 kHz +1 MHz). Also, Ebrahiminia et al. (18, 19) studied the inertial cavitation activity by dual frequency protocol (40 kHz + 1 MHz) with chemical dosimetry.

Recombinant tissue plasminogen activator (rtPA) is the standard of care for the treatment of acute ischemic stroke and was approved by US Food and Drug Administration (FDA) in 1996 (20). Echogenic liposomes (ELIPs) loaded with rtPA encapsulate both the gas bubble and rtPA (21). Destruction of ELIPs by fragmentation or acoustically driven diffusion causes both gas and drug release. ELIPs could be imaged using B-mode and the release of drug could be monitored and guided using images. There is no known specific or optimized ultrasound exposure protocol for ELIPs and both kHz (22-24) and MHz (21,25-27) radiation frequency were used. This is due to bubble sizes in ELIPs range from several nanometers to micrometers (24). As mentioned earlier, in kHz protocols, exposure is not localized and dual frequency protocols are suggested. To investigate this possibility, in this study we compare the destruction of ELIPs by three frequency protocols including 130 kHz, 1 MHz and dual frequency (130 kHz+1 MHz) using loss of echogenity.

Materials and methods

Hydrogenated phosphatidylcholine (LIPOID S PC-3) and fat free soybean phospholipids with 70% phosphatidylcholine (LIPOID S 75) were obtained from Lipoid (Lipoid Germany). Recombinant tissue plasminogen activator rtPA (Actilyse: Boehringer Ingelheim, Germany) was used (1000 µg/ml). It was frozen at -70°C until use. Other studies reported no enzymatic reduction (28, 29).

ELIPs were prepared by the pressure-freezing method (30). Phosphatidylcholine/hydrogenated phosphatidylcholine/cholesterol (45/45/10 molar ratio) was dissolved in chloroform. Chloroform was removed by rotary evaporation (under vacuum) and a thin lipid film was formed on the sides of the round bottom flask. To remove residual chloroform, the film was stored in a water bath at 50 ˚C for about 8 -12 hours. The film was hydrated by adding rtPA and agitating (10 mg lipid /ml rtPA). Liposomes were formed in this step. Liposomes were sonicated for 2 minutes (Ultrasonic Cleaner, CD-4820 model, CODYSON, China). Next, an equal volume of mannitol solution (0.32 M in distilled water) was added. The suspension contained 5 mg lipid /ml and 500 µg rtPA/ml. 1 ml aliquots of suspension were transferred to 5 ml vial with silicon cap. The vial was pressurized by a syringe of air to 4 atm. After 30 minutes, the vial was frozen at -70 ˚C for about 1-3 hours. The vial was thawed in environment temperature while the cap had been opened quickly. Size distribution of ELIPs particles was measured using a dynamic light scattering (DLS) instrument (Malvern Instruments Ltd., Malvern, UK).

ELIPs were sonicated using three frequency protocols: 130 kHz (PZT transducer with a center frequency of 132 kHz, 30 mm diameter and a 5 cm^2 effective radiation area (ERA) (SM3670, Shrewsbury Medical Ltd., Shropshire, UK)), 1 MHz (PZT transducer with a center frequency of 0.98 MHz with 30 mm diameter and 5 cm^2 ERA (Sonoplus 462 Enrof Nonius Co., Netherlands)) and dual frequency (130 kHz + 1 MHz). For 130 kHz, intensities were 0.01, 0.05, 0.10 and 0.20 W/cm^2. 1 MHz was exposed at 0.5, 1.0, 1.5 and 2.0 W/cm^2 and in dual protocol, all possible combination of intensities were used. In deionized water, pressure and frequency of probes were measured by calibrated PVDF-type hydrophone (PA124, Precision Acoustics Ltd., Dorchester, Dorset, UK) at different positions. Maximum pressures were found at 1 cm for 130 kHz and at 2.5 cm for 1 MHz from the face of probes. Fig. 1 shows the experimental set-up used in this study that kHz and MHz probes were aligned perpendicular to each other. The sample was placed at 1 cm from 130 kHz probe (near field depth) and at 2.5 cm from 1 MHz probe (one of maximum pressure locations on axial distance). Imaging transducer was placed at the nearest point relative to sample position while it was out of two ultrasound exposure fields. The walls in front of the probes were covered by a sheet of carbon foam as a sound absorber. Exposures were performed in gel phantom. Gel phantom consisted of 14% gelatin, 3% formaldehyde and 83% distilled water (31). Gelatin (ordinary and flavorless) was dissolved in 90 °C water on the stirrer. After being cooled to 40 °C, formaldehyde (Doctor Mojallali Chemical Complex, Tehran, Iran) was added and mixed slowly (no bubbles form) and poured to frame of exposure model. In gelatin, a cavity for sample was created simply by placing a 1.5 ml micro tube (conical bottom) at sample position before pouring gelatin to frame. After cooling at 5°C, the microtube was removed and the cavity for sample volume was provided.

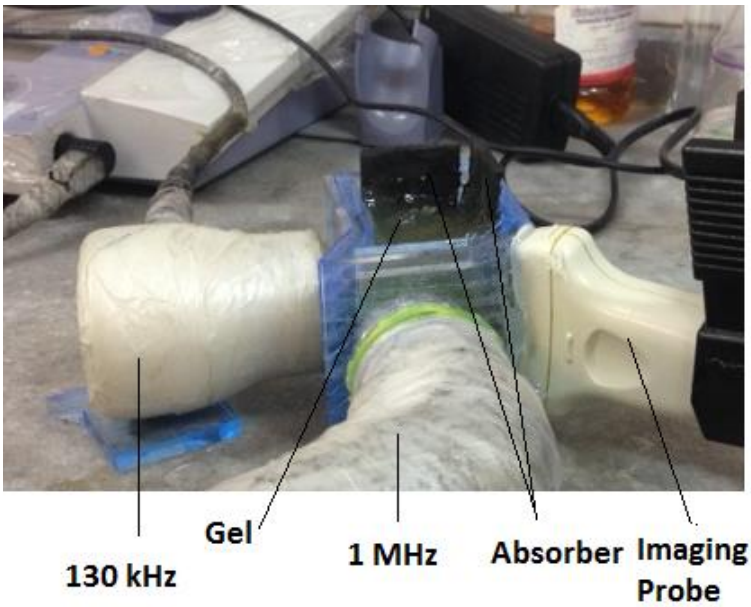

Fig 1. The experimental set up was used for imaging of samples and dual frequency sonication. Samples were transferred to micro tube shaped cavity (1.5 mL and approximately 4.0 cm length and 1.0 cm diameter) positioned at 1 cm from 130 kHz probe and at 2.5 cm from 1 MHz probe. Imaging probe was placed at the nearest point to sample while it was out of two kHz and MHz destructive fields.

ELIPs were imaged with a 10 MHz ultrasound machine (Sonix Touch ultrasound system, Ultrasonix Medical Corporation, Richmond, ON, Canada). This system did not provide specific value for mechanical index (MI) and just showed that MI was lower than a value. For all imagings, depth of scan were set to 5 cm, no focus were used and MI<0.42. ELIPs were diluted to 0.05 mg lipid/ml (rtPA concentration of 5 µg/ml) with 0.5% bovine serum albumin (BSA). 1 ml of diluted ELIPs was transferred to the cavity in gel phantom. Before ultrasound exposure by two probes, ELIPs were imaged. They were echogenic. Then ELIPs were sonicated for 10 s continuously. Coincidentally, imaging was performed. Consecutive images were recorded in AVI format. AVI videos were transferred to the computer and their frames were extracted in MATLAB (Math Works, Natick, MA, USA). On each frame a region of interest (ROI) was chosen and the mean of grayscale values (MGV) was calculated. MGVs of all frames were normalized to MGV before sonication. The MGV was measured in all frames before, during and after destructive sonication. Due to induced artifact (because of acoustic interference from the exposure fields) during destructive sonication, for each protocol, just MGVs before and after sonication were compared. In order to study the destructive effect of diagnostic pulses on echogenity, the stability of ELIPs was imaged without destructive radiation. BSA was also imaged to study its echogenity.

Statistical analysis was performed on B-mode image data acquired with different acoustic intensities at different frequency protocols for three independent runs, separately. All data are expressed as mean ± standard deviation (SD). Paired sample t-test was performed on echogenity data acquired before and after sonication with a significance level of the p-

value<0.05. The lowest intensity with a significant difference in echogenity was chosen as the destructive intensity at each frequency protocol. The statistical analysis was performed using the SPSS software package (SPSS V. 16, Inc. Chicago, IL, USA).

Results

Two peaks of intensity were shown by dynamic light scattering. The maximum peak was at 3947 nm with 92.2 % intensity and the second peak was at 133.6 nm with 7.8 % intensity (Fig. 2). The polydispersity index of 0.51 showed wide particle size distribution. Paul et al (2014) (32) observed that polydispersity indices were high (0.63-1.0) which is an indication of a large range of sizes for liposomal formulations.

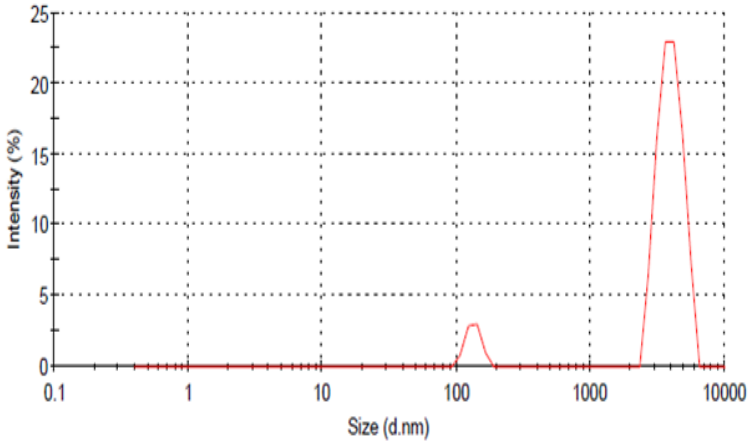

Fig. 2. Size distribution of ELIPs using dynamic light scattering

Echogenity of the BSA and ELIPs high concentration (5 mg lipid/ml) is shown in Fig. 3. We calculated the mean of echogenity in a ROI. ELIPs were 6 times brighter than BSA. This difference was also clear from the visual inspection of images. Independent-samples t-test analysis showed a significant difference for MGV between BSA and ELIPs high concentration groups (p-value<0.05).

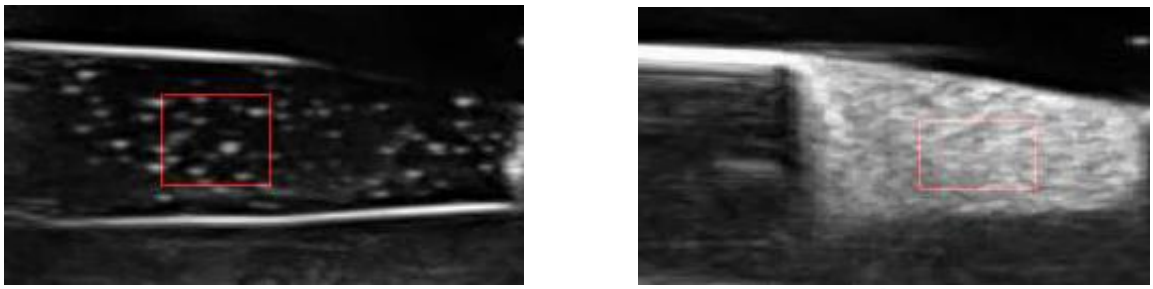

(a) (b)

Fig. 3. B-mode image of: a) bovine serum albumin (BSA) and, b) high concentration of ELIPs.

The results of sonication for ELIPs at 0.05 mg lipid/ml concentration using 130 kHz (at 0.01, 0.05, 0.10 and 0.20 W/cm^2) and 1 MHz ultrasound (0.5, 1.0, 1.5 and 2.0 W/cm^2) before and after sonication is shown in Fig. 4. Fig. 4a shows that by applying 130 kHz ultrasound waves at all intensities there would be an 80% decrease for MGV. In this regard, 130 kHz ultrasound waves induce fragmentation. Dependent sample t-test analysis of MGV between unsonicated and sonicated groups showed a significant difference in all four intensities (0.01, 0.05, 0.10 and 0.20 W/cm^2) (p-value<0.05). The increasing intensity of kHz source does not imply more fragmentations and 0.01 W/cm^2 is considered as the fragmentation threshold (minimum achievable intensity in this research) by 130 kHz ultrasound field. Fig. 4b demonstrates the results of applying 1 MHz ultrasound fields on ELIPs. Although the statistical analysis (p-value<0.05) shows significant differences between unsonicated and sonicated groups, but 40% decline in MGV can be observed. This means that 1 MHz ultrasound waves could not fragment ELIPs as much as 130 kHz waves. Increasing the intensity of MHz source does not induce a significant change in normalized MGV among groups with different intensities.

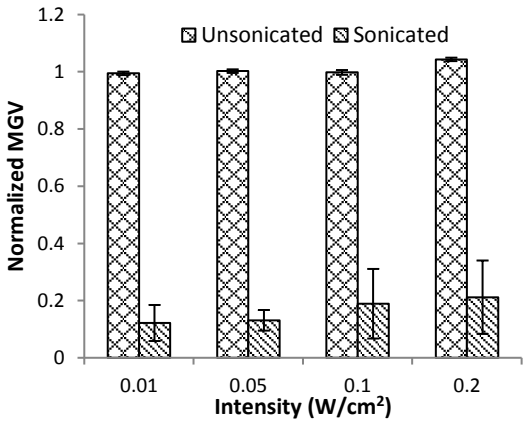

(a)

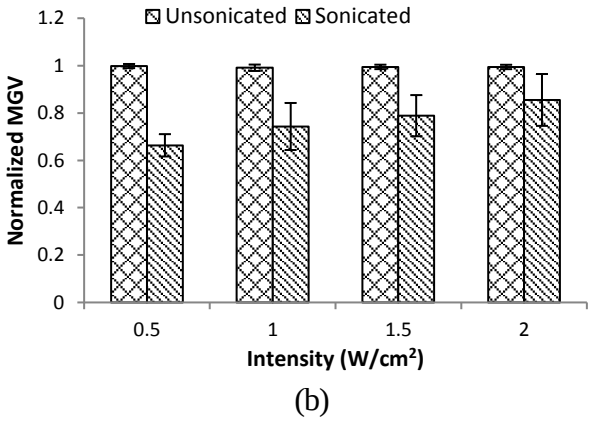

(b)

Fig. 4. Normalized mean of grayscale values (MGV) for unsonicated and sonicated ELIPs using: a) 130 kHz probe (0.01, 0.05, 0.10 and 0.20 W/cm2); b) 1 MHz probe (0.5, 1.0, 1.5 and 2.0 W/cm2).

For dual frequency sonication protocol, results of all possible combinations of intensities by two kHz and MHz probes are shown in Fig. 5. In each bar plot, the intensity of 130 kHz probe was constant (0.01, 0.05, 0.10 and 0.20 W/cm^2) and all intensities of 1 MHz probe were changed. Dual frequency protocol was suggested for localizing kHz ultrasound fields. Thus, we represent results so that effect of MHz waves (with different intensities) on each kHz ultrasound field (at finite intensity) could be investigated.

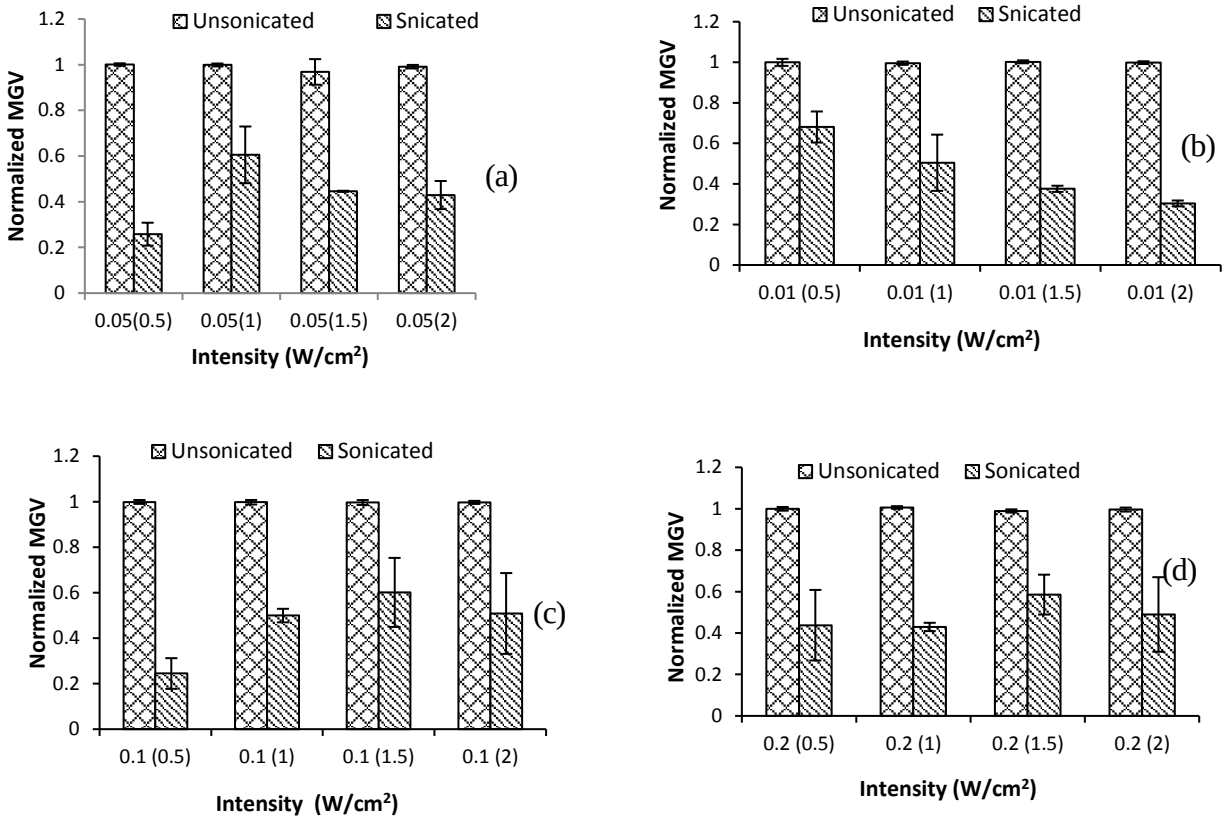

Fig. 5. Normalized MGV for unsonicated and sonicated ELIPs using; a) 130 kHz (0.01W/cm2) and 1 MHz (0.5, 1.0, 1.5 and 2.0 W/cm2); b) 130 kHz (0.05W/cm2) and 1 MHz (0.5, 1.0, 1.5 and 2.0 W/cm2); c) 130 kHz (0.1 W/cm2) and 1 MHz (0.5, 1.0, 1.5 and 2.0 W/cm2); d)130 kHz (0.2 W/cm2) and 1 MHz (0.5, 1.0, 1.5 and 2.0 W/cm2)

Although statistical analysis (p-value<0.05) shows significant differences between unsonicated and sonicated groups, but based on the results presented in fig. 5, dual frequency protocol could not decrease MGV sufficiently and consequently it could not fragment all ELIPs. Clinically, the visual inspection of ultrasound interaction with ELIPs is interesting. Visual variations of ELIPs echogenity under 130 kHz (least intensity, 0.01 W/cm^2), 1 MHz (maximum intensity, 2 W/cm^2), dual frequency (130 kHz with 0.01 W/cm^2 and 1 MHz with 2.0 W/cm^2) and diagnostic imaging pulses (stability test) are shown in Fig. 6.

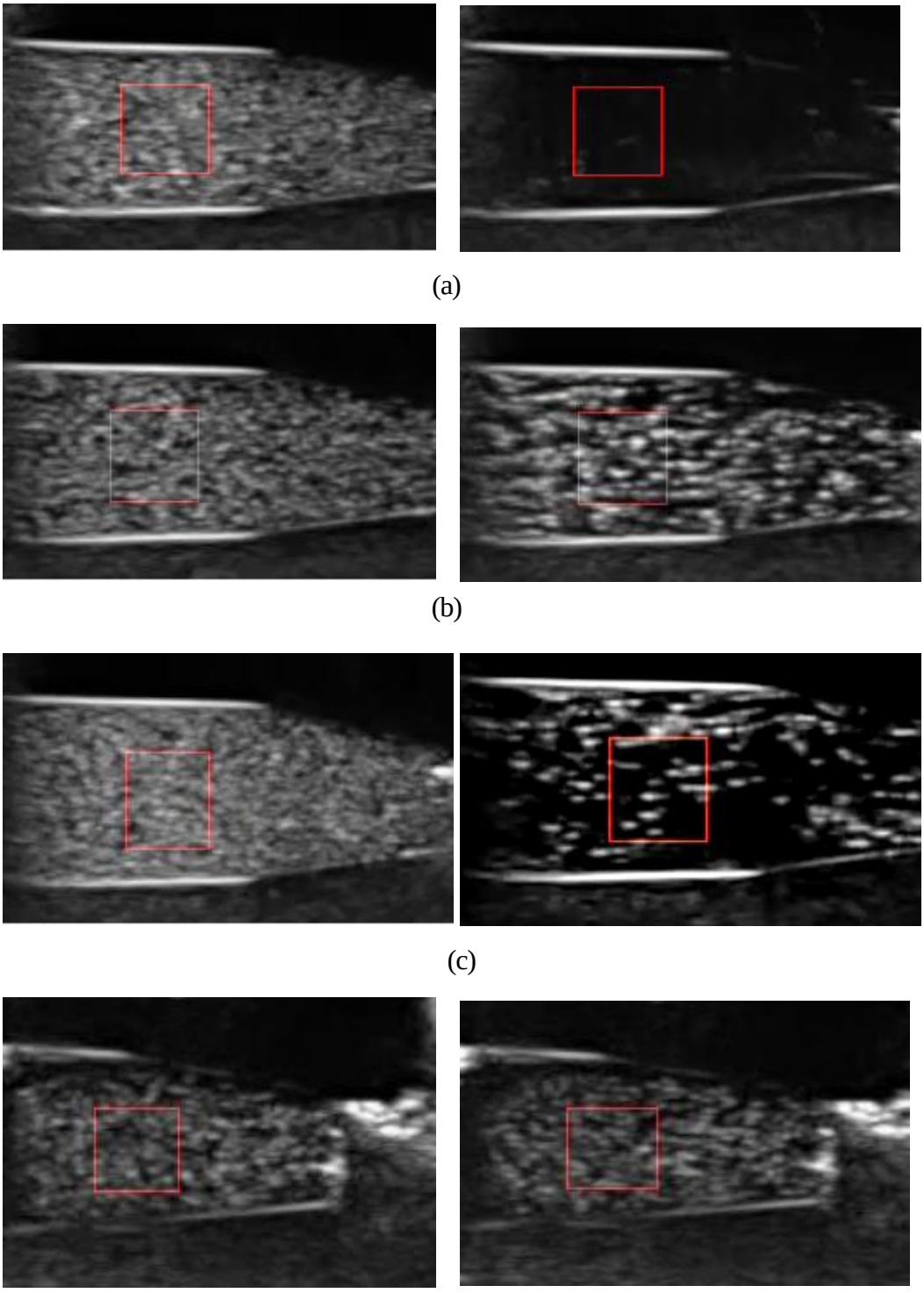

Fig. 6. Echogenity variation before (left) and after (right) different sonication protocols; a) 130 kHz (0.01 W/cm2); b) 1 MHz (2 W/cm2); c) dual frequency (130 kHz (0.01 W/cm2) and 1 MHz (2 W/cm2); d) diagnostic pulses.

After applying 130 kHz field at 0.01 W/cm^2, the initial MGV fell off to the background (Fig. 6a). This shows that almost all bubbles were fragmented and destructed. By applying 1 MHz ultrasound field at 2 W/cm^2 (Fig. 6b) and

dual one at 0.01 W/cm^2 (130 kHz)+2 W/cm^2 (1 MHz) (Fig. 6c), MGV declined but much lower than 130 kHz protocol. This indicates that some bubbles remain intact and echogen and some join to each other and form bigger particles. Fig. 6d shows that imaging pulses do not destruct ELIPs significantly.

Discussion

In our research we studied the destruction of ELIPs under three different frequency protocols. In each protocol, different intensities were applied. The result of dynamic light scattering shows that majority of ELIPs are micron sized. Smith et al. (24) reported a wide range of ELIPs sizes from nano to micro (most ELIPs were at 1.6 µm) using cell counter systems. This size does not imply the size of the bubble part of ELIPs. Bubble size has a large effect on choosing the destructive sonication frequency and different frequency protocols including kHz (21-23) and MHz (24-27). ELIPs were diluted by 5% BSA. The significant difference between echogenity of ELIPs and BSA samples shows that ELIPs entrap air enough. Echogenity is proportional to backscatter of imaging pulse at the liquid- gas interfaces due to the acoustic impedance mismatch.

Porter et al. (2006) (9) presented the echogenity reduction method to define different thresholds for fragmentation and acoustically driven diffusion. If the echogenity reduces to 10 % of initial value in less than 5 s, bubbles will be considered fragmented. In acoustic derived diffusion, this reduction lasts longer. Smith et al. (10) found fragmentation and acoustic derived diffusion thresholds for ELIPs in diagnostic frequency protocols at different pulse durations (PD) and pulse repetition frequencies (PRF). The thresholds were dependent on PD and PRF and the least pressure of 0.5 MPa was reported (1.25 kHz pulse repetition frequency, 30 s time exposure, 6 MHz using duplex Doppler). In the current study, continuous sonication was used and threshold pressure was much lower. The 130 kHz sonication destructs ELIP at low Intensity (0.01 W/cm^2 equal to 0.01 MPa). Visual inspection shows that two other protocols for all combinations of intensities could not rupture all of ELIPs like kHz. The maximum pressure used by 1 MHz probe was 0.17 MPa. Imaging of ELIPs under destructive ultrasound exposures shows that, in both 1 MHz and dual protocols, some ELIPs destruct, some keep their positions and some join to each other. Destruction at kHz may be explained by cavitation threshold because at kHz protocols cavitation threshold is low for a wide range of bubble sizes (13). Conversely, at MHz and just for narrow distribution of bubble sizes, higher pressure is required.

This study has several limitations. First, this work was performed in gel phantom (in vitro study), and does not replicate the real in vivo conditions. In dual frequency protocol, both ultrasound systems were started together manually, which may cause unknown delay between two destructive waves. This delay affects wave interference and if kHz probe starts sooner, ELIPs destruction happens which may not be due to dual protocol. In addition, induced artifacts in imaging prevented gaining echogenity in each image frame and, therefore, it was not possible to classify 130 kHz destruction as fragmentation or acoustic derived diffusion like the study conducted by Porter et al. (2006) (9).

Conclusion

This study demonstrates that kHz protocol may be more efficient in ELIPs fragmentation relative to MHz and dual frequency protocols. But due to high cavitation probability and

nonlocalized effects, kHz protocol should be controlled. Also, for better results in dual frequency protocols, frequency and phase parameters should be optimized.

Acknowledgment

This study was approved by the faculty of Medical Sciences, Tarbiat Modares University. Also, it was supported in part by the Iran National Science Foundation (INSF).

Conflicts of interest

None declared.

References

1. Frinking PJ, Cespedes EI, Kirkhorn J, Torp HG, de Jong N. A new ultrasound contrast imaging approach based on the combination of multiple imaging pulses and a separate release burst. IEEE Trans Ultrason Ferroelectr Freq Control 2001; 48(3):643–51.
2. Wei K, Jayaweera AR, Firoozan S, Linka A, Skyba DM, Kaul S. Quantification of myocardial blood flow with ultrasound-induced destruction of microbubbles administered as a constant venous infusion. Circulation 1998; 97(5):473-83.
3. Unger EC, McCreery TP, Sweitzer RH, Caldwell VE, Wu Y. Acoustically active lipospheres containing paclitaxel: a new therapeutic ultrasound contrast agent. Invest Radiol 1998; 33(12):886–92.
4. Chomas JE, Dayton P, Allen J, Morgan K, Ferrara KW. Mechanisms of contrast agent destruction. IEEE Trans Ultrason Ferroelectr Freq Control 2001; 48(1):232–48.
5. Raymond JL, Luan Y, Peng T, Huang SL, McPherson DD, Versluis M, et al. Loss of gas from echogenic liposomes exposed to pulsed ultrasound. Phys Med Biol 2016; 61(23):8321-39.
6. Chen WS, Matula TJ, Brayman AA, Crum LA. A comparison of the fragmentation thresholds and inertial cavitation doses of different ultrasound contrast agents. J Acoust Soc Am 2003; 113(1):643–51.
7. Bouakaz A, Versluis M, de Jong N. High-speed optical observations of contrast agent destruction. Ultrasound Med Biol 2005; 31(3):391–99.
8. Postema M, Bouakaz A, Versluis M, de Jong N. Ultrasound-induced gas release from contrast agent microbubbles. IEEE Trans Ultrason Ferroelectr Freq Control 2005; 52(6):1035–41.
9. Porter TM, Smith DAB, Holland CK. Acoustic techniques for assessing the Optison destruction threshold. J Ultrasound Med 2006; 25(12):1519–29.
10. Smith DA, Porter TM, Martinez J, Huang S, MacDonald RC, McPherson DD, et al. Destruction thresholds of echogenic liposomes with clinical diagnostic ultrasound. Ultrasound Med Biol 2007; 33(5):797–809.
11. Radhakrishnan K, Bader KB, Haworth KJ, Kopechek JA, Raymond JL, Huang SL, et al. Relationship between cavitation and loss of echogenicity from ultrasound contrast agents. Phys Med Biol 2013; 58(18): 6541–63.
12. Neppiras EA. Acoustic cavitation. Phys Rep 1980; 61(3):159–251.
13. Apfel RE, Holland CK. Gauging the likelihood of cavitation from short-pulse, low-duty cycle diagnostic ultrasound. Ultrasound Med Biol 1991; 17(2):179–85.

14. Saletes I, Gilles B, Bera JC. Promoting inertial cavitation by nonlinear frequency mixing in a bifrequency focused ultrasound beam. Ultrasonics 2011; 51(1):94–101.

15. Sokka SD, Gauthier TP, Hynynen K. Theoretical and experimental validation of a dual-frequency excitation method for spatial control of cavitation. Phys Med Biol 2005; 50(9):2167–79.

16. Hasanzadeh H, Mokhtari-Dizaji M, Bathaie SZ, Hassan ZM, Nilchiani V, Goudarzi H. Enhancement and control of acoustic cavitation yield by low-level dual frequency sonication: a subharmonic analysis. Ultrason Sonochem 2011; 18(1):394–400.

17. Barati AH, Mokhtari-Dizaji M, Mozdarani H, Bathaie Z, Hassan ZM. Effect of exposure parameters on cavitation induced by low-level dual-frequency ultrasound. Ultrason Sonochem 2007; 14(6):783-9.

18. Ebrahiminia A, Mokhtari-Dizaji M, Toliyat T. Dual frequency cavitation event sensor with iodide dosimeter. Ultrason Sonochem 2016; 28:276-82.

19. Ebrahiminia A, Mokhtari-Dizaji M, Toliyat T. Correlation between iodide dosimetry and terephthalic acid dosimetry to evaluate the reactive radical production due to the acoustic cavitation activity. Ultrason Sonochem 2013; 20(1):366-72.

20. Roth JM. Recombinant tissue plasminogen activator for the treatment of acute ischemic stroke. Proc (Bayl Univ Med Cent) 2011; 24(3):257-59.

21. Smith DA, Vaidya SS, Kopechek JA, Huang SL, Klegerman ME, McPherson DD, Holland CK. Ultrasound-triggered release of recombinant tissue-type plasminogen activator from echogenic liposomes. Ultrasound Med Biol 2010; 36(1):145–57.

22. Shaw GJ, Meunier JM, Huang SL, Lindsell CJ, McPherson DD, Holland CK. Ultrasound-enhanced thrombolysis with tPA-loaded echogenic liposomes. Thromb Res 2009; 124(3):306–10.

23. Bader KB, Bouchoux G, Peng T, Klegerman ME, McPherson DD, Holland CK. Thrombolytic efficacy and enzymatic activity of rt-PA-loaded echogenic liposomes. J Thromb Thrombolysis 2015; 40(2):144–55.

24. Shekhar H, Bader KB, Huang S, Peng T, Huang S, McPherson DD, et al. In vitro thrombolytic efficacy of echogenic liposomes loaded with tissue plasminogen activator and octafluoropropane gas. Phys Med Biol 2017; 62(2):517-38.

25. Tiukinhoy-Laing SD, Huang S, Klegerman M, Holland CK, McPherson DD. Ultrasound-facilitated thrombolysis using tissue-plasminogen activator-loaded echogenic liposomes. Thromb Res 2007; 119(6):777–84.

26. Laing ST, Moody MR, Kim H, Smulevitz B, Huang SL, Holland CK, et al. Thrombolytic efficacy of tissue plasminogen activator-loaded echogenic liposomes in a rabbit thrombus model. Thromb Res 2012; 130(4):629-35.

27. Hua X, Zhou L, Liu P, He Y, Tan K, Chen Q, et al. In vivo thrombolysis with targeted microbubbles loading tissue plasminogen activator in a rabbit femoral artery thrombus model. J Thromb Thrombolysis 2014; 38(1):57-64.

28. Jaffe GJ, Green GDJ, Abrams GW. Stability of Recombinant Tissue Plasminogen Activator. Am J Ophthalmol 1989; 108(1):90–1.

29. Shaw GJ, Sperling M, Meunier JM. Long-term stability of recombinant tissue plasminogen activator at -80 C. BMC Res Notes 2009; 2:117.

30. Huang SL, McPherson DD, MacDonald RC. A method to co-encapsulate gas and drugs in

liposomes for ultrasound-controlled drug delivery. Ultrasound Med Biol 2008; 34(8):1272–80.

31. Mokhtari-Dizaji M. Tissue-mimicking materials for teaching sonographers and evaluation of their specifications after three years. Ultrasound Med Biol 2001; 27(12):1713-16.

32. Paul S, Russakow D, Nahire R, Nandy T, Ambre AH, Katti K, et al. In vitro measurement of attenuation and nonlinear scattering from echogenic liposomes. Ultrasonics 2012; 52(7):962-9.